International Journal of Mass Spectrometry 298 (2010) 45–54

Contents lists available at ScienceDirect

International Journal of Mass Spectrometry

journal homepage: www.elsevier.com/locate/ijms

# Planar differential mobility spectrometer as a pre-filter for atmospheric pressure ionization mass spectrometry

Bradley B. Schneider[a], Thomas R. Covey[a], Stephen L. Coy[b], Evgeny V. Krylov[b], Erkinjon G. Nazarov[b,*]

[a] MDS Analytical Technologies, 71 Four Valley Drive, Concord, Ontario L4K 4V8, Canada
[b] Sionex Corporation, 8-A Preston Ct., Bedford, MA 01730, USA

ARTICLE INFO

*Article history:*
Received 21 May 2009
Received in revised form 12 January 2010
Accepted 13 January 2010
Available online 21 January 2010

*Keywords:*
Differential mobility spectrometry
Ion mobility
Atmospheric pressure ion pre-filtering
Mass spectrometry
Modeling

ABSTRACT

Ion filters based on planar DMS can be integrated with the inlet configuration of most mass spectrometers, and are able to enhance the quality of mass analysis and quantitative accuracy by reducing chemical noise, and by pre-separating ions of similar mass. This paper is the first in a series of papers describing the optimization of DMS/MS instrumentation. In this paper the important physical parameters of a planar DMS–MS interface including analyzer geometry, analyzer coupling to a mass spectrometer, and transport gas flow control are considered. The goal is to optimize ion transmission and transport efficiency, provide optimal and adjustable resolution, and produce stable operation under conditions of high sample contamination. We discuss the principles of DMS separations and highlight the theoretical underpinnings. The main differences between planar and cylindrical geometries are presented, including a discussion of the advantages and disadvantages of RF ion focusing. In addition, we present a description of optimization of the frequency and amplitude of the DMS fields for resolution and ion transmission, and a discussion of the influence and importance of ion residence time in DMS. We have constructed a mass spectrometer interface for planar geometries that takes advantage of atmospheric pressure gas dynamic principles, rather than ion focusing, to minimize ion losses from diffusion in the analyzer and to maximize total ion transport into the mass spectrometer. A variety of experimental results has been obtained that illustrate the performance of this type of interface, including tests of resistance to high contamination levels, and the separation of stereoisomers. In a subsequent publication the control of the chemical interactions that drive the separation process of a DMS/MS system will be considered. In a third publication we describe novel electronics designed to provide the high voltage asymmetric waveform fields (SV) required for these devices as well as the effects of different waveforms.



## 1. Introduction

### 1.1. History of DMS

Differential mobility spectrometry (DMS) is a method of separating ions based on the difference between ion mobility in high and low electric fields in gases at or near atmospheric pressure [1–3]. The earliest beginnings of this device were in the Soviet Union as part of a program to develop explosives detectors in the 1980s [4]. DMS devices with different types of ionization sources, including $^{63}$Ni, surface ionization, and atmospheric pressure chemical ionization, were coupled to mass spectrometers to characterize the mobility-separated components [5–8]. Eventually, miniaturized field portable versions of DMS were developed for the analysis of volatile organic components in ambient air [9,10] using power supplies optimized for low power consumption [11,12] and their geometrical configurations took two forms, planar [7] and cylindrical [13,14].

Laboratory-based instruments without power consumption restrictions, coupled to mass spectrometers, have been constructed as integrated instruments in order to provide orthogonal separation to the mass analysis step [5,7]. The earliest version of an electrospray DMS-mass spectrometer system was reported in 1991 [15] with several adaptations to follow over the years in 1999 [16], and later [17–19].

### 1.2. Conventional Ion mobility versus differential mobility spectrometry

DMS, also referred to as high field-asymmetric waveform ion mobility spectrometry (FAIMS) [20] or Field Ion Spectrometry (FIS) [14], is a variant of ion mobility spectrometry (IMS). Conventional IMS separates ions by the difference in the time it takes for them to drift through a gas, typically at atmospheric pressure, in a con-

* Corresponding author. Tel.: +1 781 457 5413; fax: +1 781 457 5399.
*E-mail address:* egnazarov@sionex.com (E.G. Nazarov).

1387-3806/$ – see front matter © 2010 Elsevier B.V. All rights reserved.
doi:10.1016/j.ijms.2010.01.006

stant electrostatic field of low field strength applied along the axial length of a flight tube. Ions are pulsed into the flight tube and their flight times are recorded. The time-of-flight is inversely related to the mobility of an ion. Ions have a single motion of direction (axial) and are separated according to their mobility through the gas under these low field conditions ($E < 1000$ V/cm). The drift time and thus mobility is a function of the reduced mass, charge state and shape of an ion through its interactions with the background gas. The subject has been reviewed [21–23] and the theory has been rigorously documented in Mason and McDaniel's classic text "*Transport Properties of Ions in Gases*" [24].

DMS differs from IMS in the geometry of the instrumentation and adds an additional dimension to the parameters which characterize ion separation by utilizing the field dependence of the coefficient of ion mobility known from ion transport theory. RF voltages, often referred to as separation voltages (SV), are applied across the ion transport channel, perpendicular to the direction of the transport gas flow, as shown in Fig. 1a. Due to the difference between high and low field ion mobility coefficients, ions will migrate toward the walls and leave the flight path unless their trajectory is corrected by a counterbalancing voltage, a DC potential often referred to as a compensation voltage (CV). Instead of recording the flight time of an ion through the chamber, the voltage required to correct the trajectory of a particular ion is recorded for a range of SV amplitudes. Ions are not separated in time as with an IMS. The ion mobility coefficient is encoded in the compensation voltage used to correct the tilt in ion trajectory for each SV amplitude. As such, ions are not pulsed into the analyzer but instead are introduced in a continuous fashion. The compensation voltage is scanned to serially pass ions according to their differential mobility, or set to a fixed value to pass only the ion species with a particular differential mobility.

A number of publications in the literature describe ion separations by differential mobility [5,7,9,20,25], and monographs on the subject have appeared recently [2,3]. As a result, we only provide an abbreviated phenomenological description of DMS operating principles. In DMS, ion separation occurs through the field dependence of ion mobility, symbolically represented by the alpha parameter

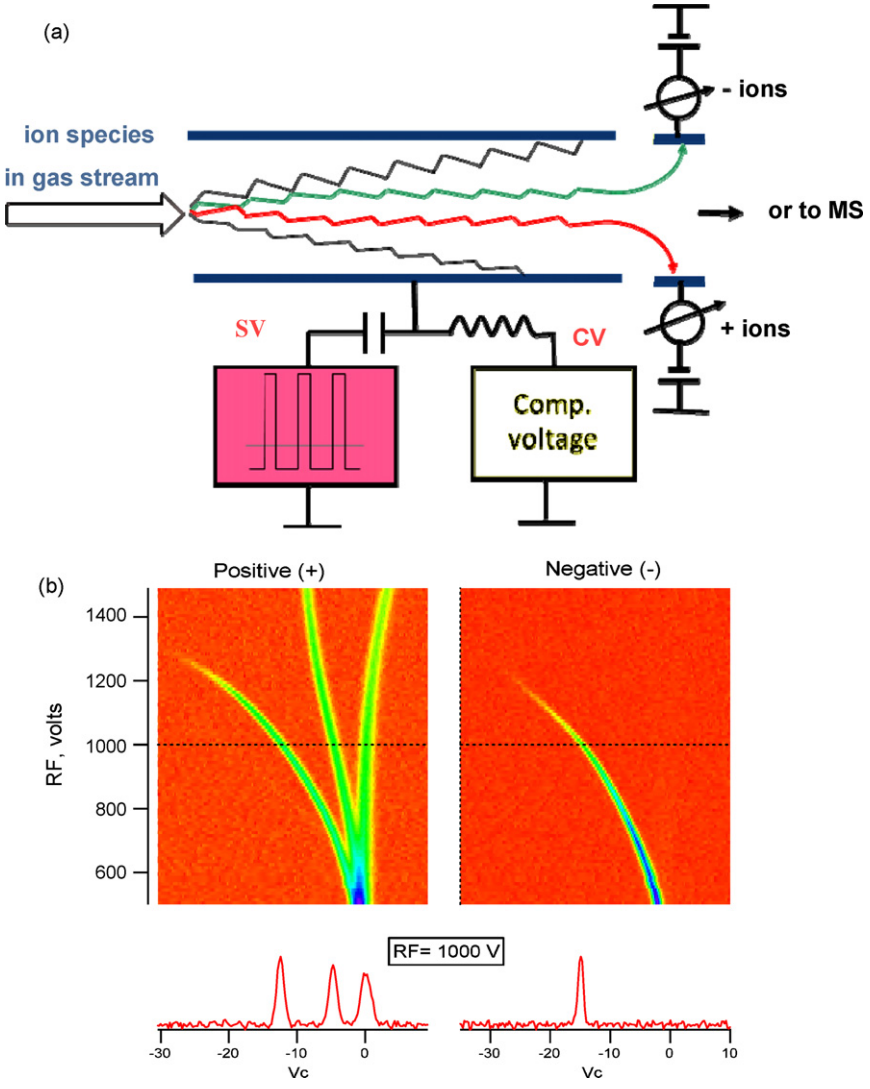


**Fig. 1.** Schematic of DMS ion filter and sensor operation. Ions generated in an atmospheric pressure ion source are carried in a transport gas through a DMS analysis region of applied fields (separation voltage SV, and compensation voltage CV), and then detected at Faraday plate detectors. (b) Dispersion plots, recorded for dimethyl methylphosphonate (DMMP). In this experiment, SV (vertical) was scanned between 500 and 1500 V and CV (horizontal) between −40 and +10 V. Positive ions (left) and negative ions (right) were recorded simultaneously. Positive ions are separated into three ion species: reactant ions peak (RIP), DMMP monomer, and DMMP dimer. Right frame shows negative background ion behavior.

in $K_i(E) = K_i(0)[1 + \alpha_i(E)]$, where $K_i(E)$ is the ion mobility for particular ion species as a function of electric field amplitude, and $K_i(0)$ at low voltage conditions. The alpha parameter can also be written as $\alpha_i(E) = \Delta K_i/K_i(0)$ indicating that it is determined by the relative change in ion mobility between low and high electric field conditions, $\Delta K = K(E) - K(0)$. Both the magnitude and sign of alpha as a function of field are important for ion species identification. The trajectory of each ion species is determined by the coefficient of mobility, the flow velocity and the alpha parameter over the entire RF waveform (SV), and by the compensation voltage (CV). Certain combinations of SV and CV fields allow the target ion trajectory to pass straight through the analytical region without colliding with the electrodes. Consequently, by scanning or fixing SV and CV, DMS can operate in several modes: (a) a particular SV and CV combination can be selected, resulting in continuous filtration of particular ion species; (b) when SV is fixed and CV scanned, a linear DMS spectra can be recorded (as shown in Fig. 1b bottom, linear DMS spectra); (c) a full differential mobility scan can be recorded when the SV and CV are both synchronized and scanned, as shown in the positive and negative dispersion plots of Fig. 1b. The information in this topographic representation or dispersion plot is equivalent to a measurement of $\alpha(E)$ for all anions and cations present in the gas stream [26,27].

The additional dimension of separation present in DMS can be best understood by considering the ion motion in the constantly varying field created by the separation voltage. Each period of the waveform has a high field component ($E$ up to 30 kV/cm) toward one electrode and a low field component toward the other, the integrated time/field exposure being equal. If the mobility of the ion were the same in the high and low fields, the ion would not drift toward either electrode but would remain near the center line and move with the gas through the chamber to the detector at the exit. But this is not what happens. During the time the ion is under the influence of the low field it travels toward the wall at a velocity typical of a classical IMS separation. The velocity can be calculated knowing the voltage and applying the low field mobility constant of the ion. The low field mobility constant has been reported in the literature for many ions, and approximate values can be calculated theoretically. During the time the ion is under the influence of the high field, it travels at a different velocity toward the other electrode, a rate that cannot be predicted based on the low field mobility constant. The physical processes governing the drag of an ion through a gas in high electric fields become different from those in low fields as the field increases. The physics governing the resistance to motion of an ion in high fields is not as well developed as it is in low fields but high field mobility constants, like low field mobility constants are reproducible for a given ion, under given conditions. Thus the drift of an ion toward either electrode is based on the difference in the mobility of that ion in high and low fields and is an analytically reproducible parameter. The term differential mobility spectrometry derives from that understanding, distinguishing it from IMS.

There are many examples of coupling low field mobility and differential mobility separations with MS in the literature. Matching the beam characteristics of a combined mobility–mass spectrometer instrument is an important consideration and the primary basis upon which these two separation systems can be distinguished. Since IMS is a timed, pulsed-ion-stream technique it most naturally couples to pulsed-ion-beam mass spectrometers such as time-of-flight MS (TOF). In both cases, the flight time of ions in a pulsed packet are measured, and that time directly correlates with the molecular properties being measured, in this case mobility and mass, respectively. Because DMS is a continuous ion beam instrument it most naturally couples with continuous ion beam mass spectrometers such as quadrupole MS. In such instruments, fields are used to filter ions and flight times are irrelevant to the measurement of the molecular properties, in this case differential mobility and mass respectively. Efficient ways to adapt pulsed and continuous beam techniques have been developed [28] but generally speaking such an approach results in some compromise in duty cycle efficiency. A review of the mobility–MS field was recently published [29].

### 1.3. Analyzer geometry

Two designs of differential mobility ion filters are in common use, cylindrical [13,20] and planar [5,7]. Originally referred to as a Field Ion Spectrometer by Mine Safey Associates Inc., the cylindrical design, using curved electrodes, has become commonly described as FAIMS (field-asymmetric waveform ion mobility spectrometry). The term DMS has maintained its association with the planar designs since its earliest conception.

They are similar in many aspects but have distinct characteristics. They both are continuous beam devices and utilize high-frequency asymmetric waveforms to separate ions based upon differences in their high and low field mobilities. The cylindrical geometry provides the potential advantage of ion focusing at atmospheric pressure due to the RF fields and analyzer curvature [30,31]. Conversely DMS provides faster ion transit times and offers a transparent mode of operation that allows all ions to be transmitted without discrimination when the separation voltage is turned off, and CV set to zero. Additionally, DMS can simultaneously transmit ions of both polarities and subject each to separation based on their differential mobility constants.

FAIMS has been the most common approach for coupling to mass spectrometry primarily because of the inhomogeneity of the focusing electric field and consequent ion focusing properties. However, the advantages of DMS described above make it a compelling consideration for mass spectrometer coupling. Previous DMS/MS couplings have predominantly involved sealing a DMS analyzer onto the inlet orifice of a mass spectrometer such that the vacuum draw of the MS provides the DMS carrier gas flow [5,15,18,19]. While this approach successfully couples mobility separations with mass spectrometry, it does not provide provisions for adjustable resolution.

This paper is the first in a series of papers describing the optimization of three principle aspects of DMS/MS instrumentation. In this paper the important physical parameters of a planar DMS–MS interface including analyzer geometry, analyzer coupling to a mass spectrometer, and transport gas flow control are considered. The goal is to optimize ion transmission and transport efficiency, provide optimal and adjustable resolution, and produce stable operation under conditions of high sample contamination. A mass spectrometer interface for planar geometries will be described that takes advantage of atmospheric pressure gas dynamic principles, instead of SV focusing, to minimize ion losses from diffusion in the analyzer and ion transport into the mass spectrometer. Efficient transfer of ions from the DMS cell into the mass spectrometer inlet is achieved without the need for additional electrostatic focusing devices or modifications to the mass spectrometer inlet orifice. Other important considerations such as optimization of voltage frequency and amplitude, and ion residence time within the DMS fields will be discussed in the context of providing optimal and adjustable resolution and transmission for ions. In a subsequent publication the control of the chemical interactions that drive the separation process of a DMS/MS system will be considered [32]. In a third publication we describe novel electronics designed to provide the asymmetric SV fields at high voltages required for these devices as well as the effects of different waveforms [33].

## 2. Experimental

### 2.1. Instrumentation and chemicals

The mass spectrometer used for these studies was a prototype API 5000™ (AB/MDS Analytical Technologies, Foster City, CA) having a 600 μm inlet aperture and a total gas throughput of 3.5 L/min from atmosphere to vacuum. Ion source region of the mass spectrometer was modified for incorporation of various DMS analyzers. The standard ceramic orifice plate was replaced with a modified ceramic plate that included provisions for sealing a DMS cell (variable length and dimensions) in front of the gas conductance limiting orifice. The standard curtain plate was replaced with a modified curtain plate that protruded further from the orifice plate such that DMS cells could be installed within the curtain chamber space. The increased protrusion of the curtain plate from the inlet necessitated an extension flange mounted between the standard Turbo V™ ion source and the mounting flange on the front of the instrument. A number of different extensions were designed to provide variable offsets for DMS cells with different lengths. The standard Turbo V™ ion source was used without further modification. DMS electrodes were constructed from hemispherical pieces of stainless steel, and were mounted in holders constructed from either Teflon or ceramic materials. Vacuum seals were maintained between the DMS cells and mass spectrometer inlet using Teflon gaskets or by providing lapped sealing surfaces on both the DMS cell and mass spectrometer inlet.

The separation voltage was provided using either a clipped sinusoidal waveform from a "flyback" generator (SIONEX, Bedford MA) or a bisinusoidal waveform from a custom tuned-harmonic generator [11,34]. The clipped sinusoidal waveform was designed for low power consumption applications and operated with a fixed frequency of 1.25 MHz and mean-to-peak amplitude range of 0–1500 V. The bisinusoidal waveform generator could be operated with adjustable frequency spanning a range of approximately 750 kHz to 3 MHz, with mean-to-peak amplitudes from 0 to 3333 V (5000 V peak-to-peak). The separation voltage was delivered to the DMS electrodes using shielded coaxial cable either through the source housing, or via high voltage feedthroughs mounted into the back of the curtain chamber.

Samples of minoxidil, safranin orange, buspirone, reserpine, calibration peptide, ephedrine, pseudoephedrine, and leucine were purchased from Sigma Chemical Co (St. Louis, MO). For infusion experiments, samples were diluted in solvent comprising 50/50 methanol/water with 0.1% formic acid (Fischer Scientific, Nepean, ON). Hank's Buffer solution was purchased from Sigma Chemical Co. (St. Louis, MO) and was prepared using the manufacturer's specified procedure.

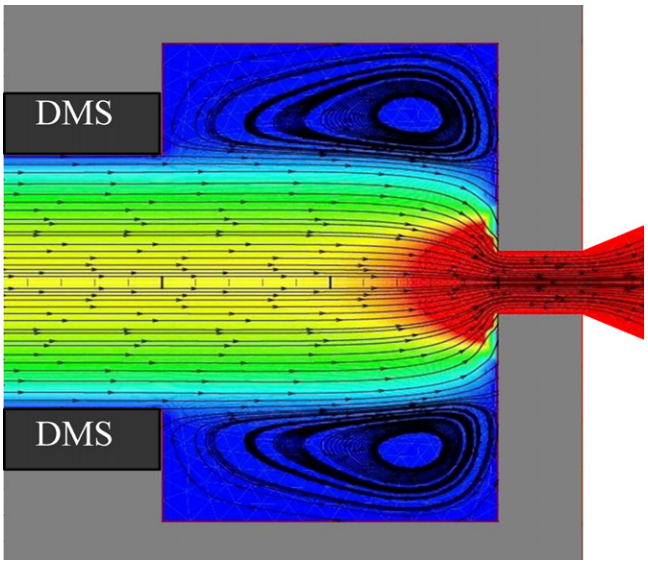


**Fig. 2.** CFD generated gas flow velocity and streamlines at DMS–MS transition. Modeling results demonstrate gas flow streamlines in the region bounded by a DMS exit and the inlet orifice of a mass spectrometer. The DMS section has a 1 mm gap and is sealed to a 0.25 mm inlet orifice, with a wider diameter chamber separating the DMS and the MS orifice.

### 2.2. Software and data processing

The mass spectrometer and DMS separation and compensation fields were controlled by a custom version of Analyst 1.4.2 updated with full integration of DMS control. The software provided an accessible range of separation voltage from 0 to 5000 V peak-to-peak. The compensation voltage was adjustable from −100 to +100 V, and the voltage differential between the DMS cell and the inlet orifice was adjustable from −100 to +100 V.

The data in Table 1 showing diffusion losses, residence times, and FWHM values with different cell geometries and gas flows were calculated using software created by Sionex making use of a series solution to diffusion in the plug flow limit, as well as the Einstein–Nernst relationship between mobility and diffusion.

The simulations of gas flow streams in Fig. 2 were calculated using a computational fluid dynamics flow solver, CFD++, developed by Metacomp Technologies, to solve the compressible axisymmetric form of the Navier–Stokes equations. The parameters and assumptions utilized are described in Jugroot et al. [35], where solutions to ion transport problems in the atmospheric ion sampling region of a mass spectrometer are detailed.

**Table 1**
Calculated data describing the relationship between cell geometry, gas flow, ion residence time, diffusion losses expressed as coefficient of transmission, and resolution expressed as full width half maximum in volts.

| | Height (*H*) (mm) | Length (*L*) (mm) | Width (*W*) (mm) | Gas flow (L/min) | Residence time (ms) | Coefficient of transmission | FWHM (V) |
|---|---|---|---|---|---|---|---|
| Group 1 | 1 | 30 | 10 | 3.5 | 5.1 | 0.79 | 2.19 |
| Group 1 | 1 | 30 | 10 | 2.5 | 7.2 | 0.73 | 1.63 |
| Group 1 | 1 | 30 | 10 | 1.5 | 12.0 | 0.62 | 1.06 |
| Group 1 | 1 | 30 | 10 | 0.5 | 36.0 | 0.29 | 0.52 |
| Group 2 | 1 | 10 | 10 | 3.5 | 1.7 | 0.91 | 6.10 |
| Group 2 | 1 | 20 | 10 | 3.5 | 3.4 | 0.85 | 3.17 |
| Group 2 | 1 | 30 | 10 | 3.5 | 5.1 | 0.79 | 2.19 |
| Group 2 | 1 | 40 | 10 | 3.5 | 6.9 | 0.74 | 1.70 |
| Group 3 | 0.5 | 60 | 10 | 3.5 | 5.1 | 0.47 | 0.71 |
| Group 3 | 1 | 30 | 10 | 3.5 | 5.1 | 0.79 | 2.19 |
| Group 3 | 2 | 15 | 10 | 3.5 | 5.1 | 0.93 | 8.05 |
| Group 4 | 1 | 50 | 10 | 0.3 | 100 | 0.07 | 0.38 |
| Group 4 | 1 | 584 | 10 | 3.5 | 100 | 0.07 | 0.38 |

Height is defined as the gap between the electrodes and length as the axial flight path of the ions. See Section 3.2.1 for information about the calculations.

Ion simulations during transport through a DMS cell were done using Sionex MicroDMx software; details and description are presented in reference [36]. Ion trajectories are tracked under the influence of gas flow and static and dynamic electric fields with user-definable waveform shape and frequency, and parameterized ion mobility properties. The software uses the boundary-element method to compute field distributions, and fine time steps to track ion motion. It includes the neutralization of gas-phase ions that collide with metal surfaces.

## 3. Results and discussion

### 3.1. Planar versus cylindrical geometries for mass spectrometry coupling

Although both cylindrical and planar designs use the same principle for ion filtration, they differ with respect to several operational parameters and performance metrics. The main distinguishing characteristics are described below in more detail.

#### 3.1.1. Ion residence time

In general for focusing to develop in cylindrical designs a longer residence time in the analytical region is needed, so longer electrodes are typically used. The focusing properties of cylindrical electrodes reduce the resolving properties of the varying fields. Therefore, longer residence times are used to compensate for the loss in resolution with greater losses due to diffusion occurring as a consequence. The interplay between focusing and resolution will be described further in the following section and the relationship between ion losses due to diffusion and residence time in Section 3.2.1.

Typical cylindrical designs use residence times on the order of 100 ms or longer. Flight times of this duration do not match the switching speed of a quadrupole mass spectrometer when monitoring mass transitions operating in multiple reaction or selected ion monitoring mode. This results in channel overlap otherwise referred to as channel cross-talk where a DMS separated ion will appear in more then one mass channel. This is particularly a problem when the mass spectrometer cannot separate isobaric or nearly isobaric species and DMS selectivity is required to distinguish the analytes. Flight times of less than 10 ms in the planar design allow synchronization of the DMS and mass spectrometer to occur during fast switching, as described further below.

#### 3.1.2. Resolution

The relationship between the focusing properties of a cylindrical device and resolution have been theoretically explained [1] and have been demonstrated experimentally [20]. A recent publication [19] compares planar and cylindrical designs, and shows that the selectivity of the planar design is 3–5 times better under conditions where the mobility cells were constructed to give similar residence times. This result can be understood based on the loss of dispersion caused by ion focusing. Analytical considerations and recent simulations reveal that a sharp electrode curvature is needed to achieve effective focusing in FAIMS. However, reducing curvature improves resolution and the coefficient of ion transmission through the analytical region. In conclusion, planar and cylindrical designs can achieve similar resolutions, however, planar designs require substantially lower ion residence time in the analytical region. The shorter residence time reduces diffusion losses and more efficiently matches the switching speed of a mass spectrometer when jumping between selected ion transitions.

#### 3.1.3. Transparent mode of operation

The advantage of being able to use short flight paths to minimize residence time extends to other modes of operation. With all voltages off and diffusion losses reduced to a minimum, all ions in a spectrum are transmitted in a fashion similar to there being no mobility cell installed, typically referred to as transparent mode of operation. As described in more detail in Section 3.2.1 losses from diffusion are on the order of 20–30% for planar cell geometries optimized as described here for mass spectrometry. With fields off and the same analyzer gap diameter, a cylindrical cell with residence times of 100 ms would loose up to 93% of ions due to diffusion alone with some additional losses from the curved gas flow path.

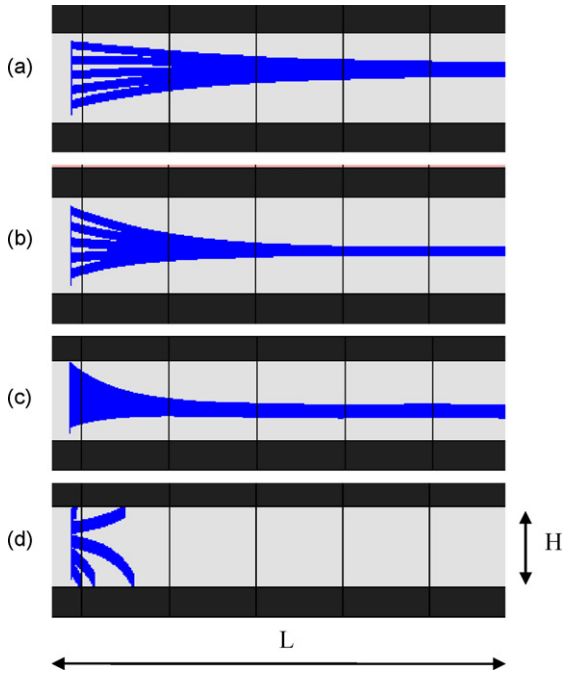


**Fig. 3.** Simulated ion focusing-defocusing properties of a cylindrical FAIMS for four different ions with different properties. A slice of the inlet section of the FAIMS cylindrical gap is shown: $L$ is length and $H$ is height of analytical channel. In each simulation (a–d), ions are injected at 5 different radial positions and are shown to be focused or defocused depending on their alpha parameter $\alpha(E)$ and effected electric field strength $E$: (a) Weak focusing $K = 1$, $\alpha(E) = 6.0 \times 10^{-6} E^2$; (b) Moderate focusing $K = 1$, $\alpha(E) = 1.2 \times 10^{-5} E^2$; (c) Strong focusing $K = 2$, $\alpha(E) = 1.2 \times 10^{-5} E^2$; (d) Defocusing $K = 2$, $\alpha(E) = -1.2 \times 10^{-5} E^2$.

#### 3.1.4. Ion focusing in FAIMS

In the cylindrical design, the transverse electric field distribution is dependent on radial position. The electric field close to the inner cylinder is stronger than that near the outer cylinder:

$$E(r) = \frac{V}{r \ln r_1/r_2},$$

where $r_1$, and $r_2$, are the radii of the inner and outer cylinders, and $r$ is the radial coordinate of an ion between the two cylinders. Ions located at different radial positions experience different electric field strengths. Therefore, the trajectory of an ion located near the periphery of the analytical gap differs from that of the same type of ion located close to the inner cylindrical electrode. Depending on the sign of the alpha parameter, and on the local SV and CV values and direction, it is possible for all ions of a particular type to be focused toward a radial position within the gap. More highly curved electrodes (with smaller $r_1$) provide a more inhomogeneous electric field and consequently provide more effective ion focusing. The first systematic discussion of ion focusing in the cylindrical geometry was presented by Krylov in 1995 [30,37]. The same focusing effects were later described by Guevremont [31] and others [38,39].

Fig. 3a–d shows a simulation of ion focusing in a cylindrical gap for 4 ion species, with different coefficients of mobility and alpha

parameters, moving in the same analytical gap, in the same transport gas flow, SV and CV [36]. To show the relative efficiency of ion focusing in each of the cases, we have presented the ion trajectories for five ions of each species, started from different radial positions between inner (bottom) and outer (top) electrodes. As shown in Fig. 3a–c, the focusing efficiency depends on the coefficient of mobility and on the value and sign of the alpha parameter and value of SV. Focusing is greater for ion species with higher mobility coefficients, higher values of the alpha parameter and for higher values of the SV voltage. Changing the sign of the alpha parameter changes ion trajectories from focusing to defocusing (Fig. 3d), as does changing the ion polarity or the SV field direction. The modeling results demonstrate that the focusing advantage of cylindrical geometry systems is not universal to all ions under a given set of conditions.

### 3.2. Optimization of transmission, resolution, and contamination control using vacuum drag as the source of transport flow

The SV focusing effect described above does not occur in DMS. However, there are additional ways to improve the transmission through a DMS cell as well as improve the transfer of ions from the cell into a mass spectrometer. Since the separation and transfer of ions occur at atmospheric pressure, considering the effect of gas flows can be more important than focusing fields. Losses of ions in transport gases at atmospheric pressure are primarily a consequence of diffusion. With planar geometries the residence time in the cell can be reduced to a few ms thus reducing diffusion losses. Transport of ions from the cell into the mass spectrometer can also be optimized using similar gas dynamic principles. Solutions to both of these issues are discussed below in the context of utilizing the mass spectrometer vacuum system as the source of transport gas flow. In addition, the implications of utilizing vacuum drag as the source of transport gas flow on contamination are discussed.

#### 3.2.1. Transmission losses through a DMS cell and the relationship between residence time, resolution, and ion losses from diffusion

The residence time of an ion in the SV field is a primary determinant of performance of planar DMS. The longer the cell or slower the gas the better the resolving power of the DMS analyzer. However, with the increased resolution come increases in ion losses as a longer time is available for diffusion losses to occur. The trade-off between resolution and transmission can be mathematically quantified with cells in a range of geometries that will provide the necessary separation fields using power supplies designed within practical engineering limits. Calculations and models were used to provide reasonable estimates of these analytical parameters and are described in Section 2.2. Table 1 shows data generated from these models illustrating the importance of these considerations. A number of the geometries and flows were experimentally tested providing results to support the calculated values.

Group 1 shows the effect of transport gas flow rate ($G$) with a cell of fixed geometry. Reducing the gas flow through the analyzer improves resolution due to a longer residence time in the separation field. However, the trade-off is lower transmission as a result of diffusion losses with longer residence times.

Group 2 shows the effect of changing one dimension of the cell, the length ($L$), and keeping all other parameters constant. Increasing the length of the cell at fixed transport gas flow is functionally the same as reducing the gas flow for a given length. As described above, this improves resolution, albeit with higher diffusion losses.

The data in Group 3 shows that ion residence time in the separation fields is not the only important consideration. Keeping the cell volume and thus residence time constant, resolution and transmission can be altering by adjusting the cell height (H-gap between electrodes) and length. Increasing the analyzer gap height improves transmission; however, residence time has to increase in order to achieve similar resolution.

The data in Group 4 demonstrates the consequences of long residence times, demonstrating severe ion losses due to diffusion. These losses occur in planar geometry DMS cells, as well as cylindrical geometry cells when the focusing condition is not met.

The data from Table 1 provide guidance towards choosing the optimal geometry for a DMS intended for a mass spectrometer interface. The final determination depends on other aspects of the MS interfacing problem, including establishing an efficient means of transporting ions from the exit of the cell into the mass spectrometer and means for dynamic resolution control of the DMS. Both will be considered in the following sections.

#### 3.2.2. Transmission losses between cell and mass spectrometer inlet

The strong flow of gas in the region immediately in front of the mass spectrometer atmosphere to vacuum aperture will efficiently transport ions from atmosphere to vacuum. Using chambers to confine the gas in this region ion transfer efficiency has been shown to be as high as 80% with nano-electrospray ion sources [40]. The small dimensions of a planar DMS cell match well with the volume of the vacuum drag region in front of the vacuum aperture potentially offering transfer efficiencies similar to those of nano-electrospray if the full force of the vacuum can be applied to the region after the exit of the DMS cell. This requires sealing a DMS cell with the appropriate geometry to the inlet orifice of the mass spectrometer and utilizing the vacuum drag as the force drawing the transport gas through the cell. This configuration has the additional benefit of simplifying construction and operation by eliminating the need to carefully control the transport gas flow at all times. With this arrangement, the interface sees a single fixed and stable flow determined by the pumping speed and size of the conductance limiting orifice of the mass spectrometer. The mass spectrometer used for these experiments has a net gas flow through the aperture of ≈3.5 L/min. The variety of cell geometries with different performance specifications listed in Groups 1–3 of Table 1 are reasonable candidates for a planar DMS cell to be interfaced to this mass spectrometer.

A more detailed consideration of the gas flows in the region in front of the mass spectrometer aperture can be visualized with computational fluid dynamic models [35]. Fig. 2 illustrates the results of modeling of the gas flow streamlines for a DMS cell with gap height approximately 4× the diameter of the mass spectrometer inlet orifice. Under these conditions, a vast majority of the gas flow streamlines converge through the orifice, entraining with them the ions exiting the DMS cell. A portion of the lowest velocity streamlines from the periphery of the gas flow impact with the walls of the orifice, potentially leading to neutralization of a portion of the ions entrained within them.

Using electrode geometries as described in Table 1, with width dimensions ($W$) on the order of 10 mm, some ion losses in the interface region are predicted from the CFD++ model when the mass spectrometer inlet orifice is ≈0.6 mm. In order to reduce these losses a technique was tested to effectively slow the ion velocity relative to the gas by applying a "braking" potential in this region. The location of this negative DC potential offset between the DMS cell relative to the downstream orifice is shown in Fig. 4. To maintain effective mobility residence time, electrode dimensions ($H \times W \times L$) were selected to be 1 mm × 10 mm × 30 mm and the effectiveness of the braking potential was evaluated for ions of various $m/z$ as shown in Fig. 5. For all of the ions that were tested in this experiment, the optimal DMS offset voltage was negative (DMS potential slightly lower than the orifice potential) to establish a braking potential. The magnitude of the optimal offset voltage and the width of the optimal voltage range both increased with the

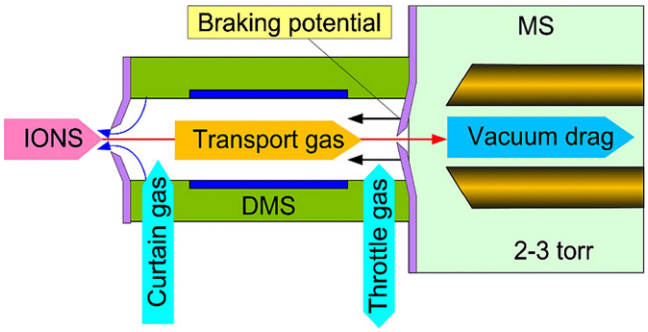


**Fig. 4.** Schematics for DMS coupling including vacuum seal to the orifice, braking potential to optimize ion coupling efficiency, and throttle gas for tunable selectivity.

$m/z$ of the ion of interest, likely reflecting the known decrease in the ion mobility constant for higher $m/z$ ions. The data in Fig. 5 demonstrate that the transfer of ions from a slotted DMS analyzer to a circular mass spectrometer inlet may be improved by slowing down the ions allowing them to be influenced by the bending gas streamlines converging on the orifice aperture.

By comparing the signal obtained with no DMS cell installed to the signal when a cell is installed, one obtains the total loss which is the sum of the diffusion losses traversing the cell and the losses in the transfer from the cell into the mass spectrometer. Infusion experiments at 10 μL/min with samples of taurocholic acid were conducted with the configuration shown in Fig. 4 and line one of Table 1 using separation voltages of 3000 Vp-p. The measured coefficient of transmission under these conditions was 0.63, in reasonable agreement with the predicted value of 0.79 shown in Table 1. The data show that the measured losses are similar to those expected from diffusion processes alone indicating that losses during the transfer are minimal with this interface. Additional losses can occur during ion filtering as a result of cluster ion formation, but they are highly dependent on the compound chemistry and sample inlet conditions. These losses are not dealt with here but will be addressed in a subsequent publication dealing with chemical effects as they can have important consequences on analytical methodologies [32].

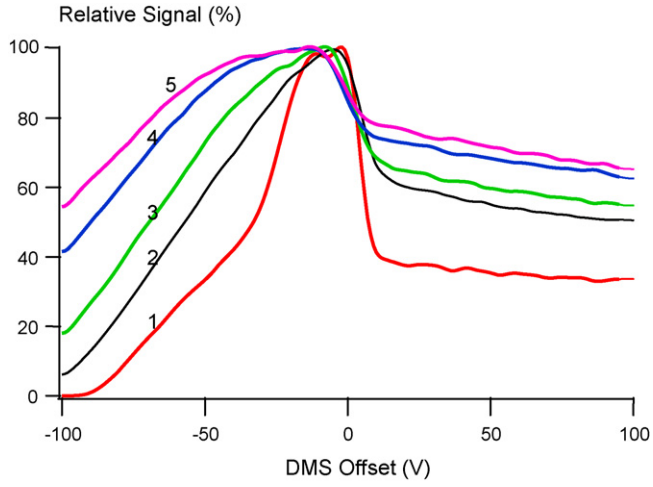


**Fig. 5.** Plots of the signal for various ions versus the DMS offset potential relative to the mass spectrometer inlet orifice. A negative DMS offset voltage establishes a braking potential between the DMS cell and mass spectrometer inlet. The masses being monitored are $m/z$ (1) 210, (2) 315, (3) 386, (4) 609, (5) 829. Larger braking potentials were optimal for ions with increasing $m/z$. In these experiments the SV was 3500 V and the CV optimal for each ion was used.

### 3.2.3. Control of resolution using a fixed gas flow generated by the vacuum system

As shown in Table 1, resolution, and thus selectivity, can be adjusted in a DMS cell in a variety of ways all of which involve increasing the residence time of ions in the SV fields. When a DMS cell of fixed dimensions is sealed onto the vacuum inlet of a mass spectrometer, the average residence time $t_R$ of ions can be calculated using equation,

$$t_R = \frac{V_{cell}}{G}$$

where $V_{cell}$ is the volume of the DMS cell ($L \times W \times H$) and $G$ is the gas flow rate into the mass spectrometer. With this approach to maximize ion transfer efficiency by using the available vacuum drag from the mass spectrometer, one means to achieve variable resolution would be by installing DMS cells with different internal volumes. DMS cells with variable volume are most conveniently created by elongating the total length of the cell ($L$) since changes to the gap height ($H$) affect the field between the analyzer plates and changes to the width of the DMS slot ($W$) can affect transmission into the vacuum system of the mass spectrometer. However, this approach for adjustable selectivity is impractical since it would require hardware modifications for different resolution settings.

A means for altering the transport gas flow is illustrated in Fig. 4. A variable flow of nitrogen gas can be added, or extracted in the chamber after the DMS cell to effectively "throttle" the transport gas flow through the DMS to a new (lower or higher) value. The residence time for ions within the DMS cell in this configuration is given by the equation,

$$t_R = \frac{V_{cell}}{G - G_T}$$

where $G_T$ is the volumetric flow rate of throttle gas provided into the juncture chamber. With this configuration the DMS mobility cell was optimized for highest sensitivity/lowest selectivity (short residence time) and then selectivity was adjusted with the throttle gas regulation. As shown in Fig. 4 the process of switching between "high resolution" and "high sensitivity" modes of operation (or in inverse direction) can be reached practically for within a few seconds and can be provided through software control. Fig. 6A–C demonstrates an example of selectivity adjustment using this approach for the separation of the diastereomers ephedrine and pseudoephedrine. With the throttle gas adjusted to provide high sensitivity and low resolution, a single peak is observed with 2 shoulders as demonstrated in Fig. 6A. Increasing the gas setting by 0.5 L/min improves resolution of the two diastereomers by narrowing the mobility peak widths as demonstrated in Fig. 6B. The structures shown in Fig. 6, show that the two compounds differ only in the orientation of a single hydroxyl group near the center of the molecular structures, and have identical masses ($m/z$ = 165.11536 Da). There is little change in the observed signal for these 2 compounds as would be expected based upon the data presented in Table 1. Further increases to the throttle gas setting provide additional enhancements to resolution such that specific CV settings can be chosen to exclusively transmit either of the 2 diastereomers, albeit with the sensitivity reduction demonstrated in Fig. 6C. When isobaric or nearly isobaric compounds have more extensive structural differences, DMS separation is generally much greater than observed for the ephedrine/pseudoephedrine system.

### 3.2.4. Contamination control using vacuum drag as the source of transport flow

In a system where the transport gas is drawn directly from the ionization region by vacuum drag forces, contamination of the DMS analyzer and mass spectrometer entrance optics could be expected. As shown in Fig. 4, the transport gas with this system is drawn from

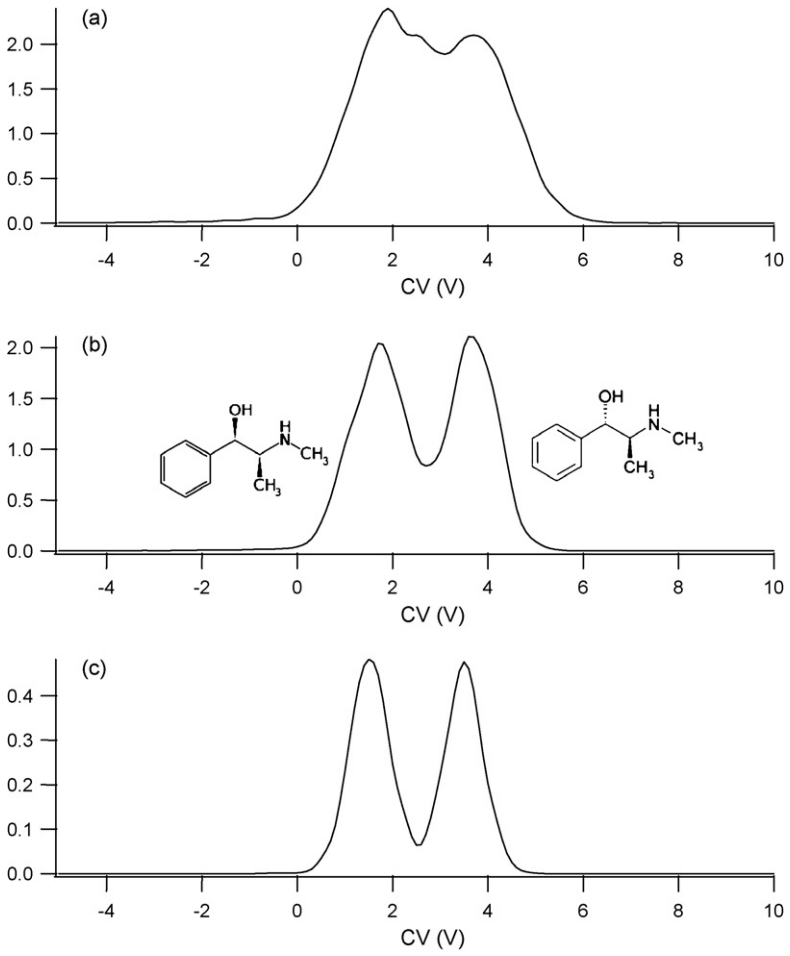


**Fig. 6.** Separation of diastereomers ephedrine and pseudoephedrine (MW = 165.11536). Increasing throttle gas supply reduces the DMS transport gas flow, increasing residence time and DMS resolution. DMS transport gas flows are (a) 2.5 L/min, (b) 2 L/min, and (c) 1 L/min. Signal ordinate is cps/$10^5$ in all panes, so relative intensity can be compared.

a larger curtain gas flow, a portion of which flows counter current to the flow of ions and sample debris. This provides sufficient protection of both analyzers to allow for long-term stable operation under conditions of severely contaminating samples.

A series of experiments were conducted to evaluate the long-term robustness of this configuration. The experiments involved repeated flow injection of approximately 20 μL of samples comprising either 10 pg/μL reserpine solution or undiluted Hank's buffer solution, a high salt content matrix used for cell cultures. Each cycle of 3 injections was comprised of 2 Hank's buffer samples and 1 reserpine sample and the decay profile for the instrumental response for the reserpine samples was tracked ($m/z$ = 609 Da) over the course of approximately 2352 total injections. The typical decay profile for this prototype instrument gave approximately 2-fold signal reduction due to curtain plate and inlet orifice contamination in the absence of the DMS cell. Repeating the same experiments with the DMS installed, the signal reduction was approximately 1.6×, demonstrating good resistance to contamination. In addition, the peak position in CV space was extremely reproducible throughout the experiment, maintaining a constant CV value to within ±0.2 V. Fig. 7A shows the stability of the peak position, and the small decrease in sensitivity during this test. Fig. 7B–D show photographs of the curtain plate (B), DMS cell entrance (D), and inside the DMS electrodes (C) at the end of these experiments. As shown in Fig. 7B, there was substantial contamination of the atmospheric side of the curtain plate as would normally be expected. The exposed portion of the DMS cell inlet and 1 mm inside the analyzer exhibited contamination but less than the curtain plate, indicating the curtain gas flow was acting to filter some debris (Fig. 7C and D). The remainder of the inside length of the electrodes was clean and served to shield the mass spectrometer orifice from contamination as well. This indicates that the transport gas, delivered in this fashion, was kept sufficiently pure to minimize deposit formation. It should be noted that an atmospheric cell of this type can be rapidly removed and cleaned with no need to break vacuum on the mass spectrometer and a requirement for more frequent cleaning than operation without the cell was not observed. For this test, it appeared that, with the cell in place, the mass spectrometer inlet orifice would require less frequent cleaning with the DMS unit mounted.

### 3.3. Voltage optimization

SV frequency and voltage also play a role in optimizing DMS resolution and transmission efficiency. A DMS analyzer installed on a laboratory-based mass spectrometer system is not limited by the traditional power consumption constraints of field portable DMS devices. Thus DMS performance can be improved by increasing the gap or operating at higher frequency, regardless of the increase in power consumption. Modifying the SV frequency changes ion transmission because the ion oscillations in the SV waveform result in wall collisions as ions enter the DMS filter region. In addition the higher the amplitude of the oscillation the lower ion transmission will be through the filter gap.

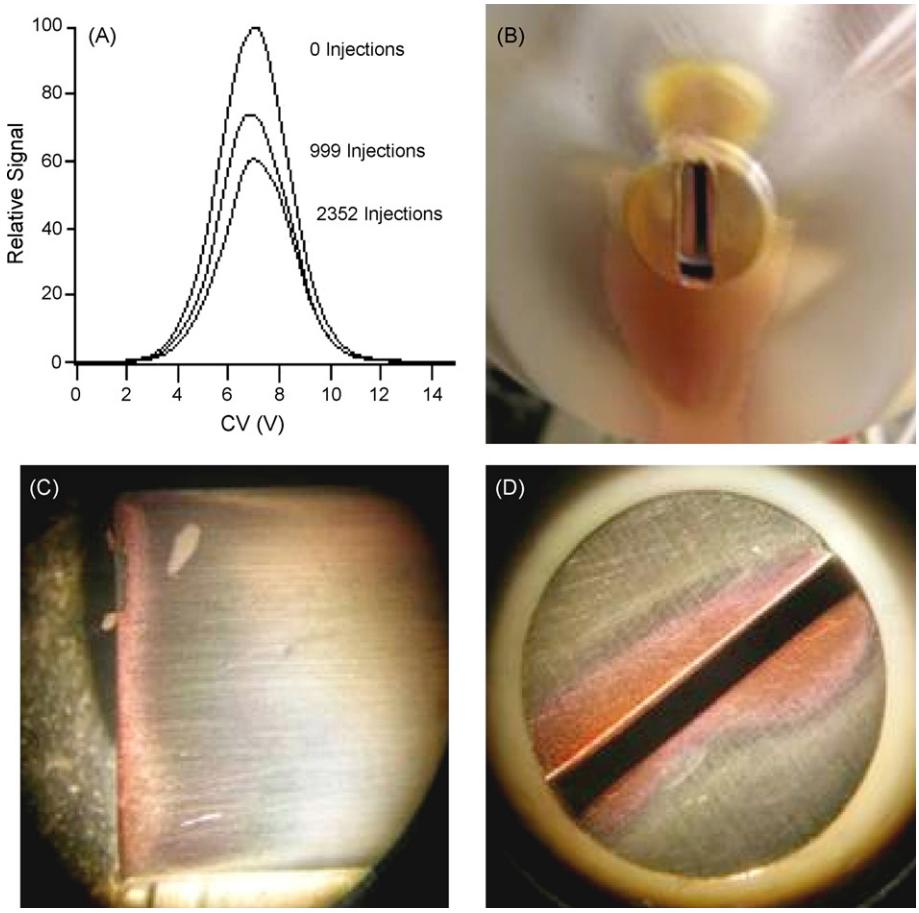


**Fig. 7.** DMS contamination test results for repeated injections of Hank's buffer and reserpine (see text for details). From top left to bottom right, (A) Signal is reduced as the number of injections increases from 0 to 2352 injections, but to a lesser degree than is observed without the DMS interface. (B–D) Photographs after 2352 sample injections of Hank's buffer + reserpine of the curtain plate (B), internal side view of DMS electrode surface (C), and DMS inlet (D).

One way to reduce these losses is to increase the frequency of the separation waveform in order to reduce the amplitude of the transverse ion oscillation, thereby decreasing wall collisions. Fig. 8 shows experimental data on leucine for two different frequencies, illustrating the reduced losses at higher SV frequencies, and computer-simulated ion trajectories [36] at two different frequencies. The modeling data displayed in the middle and bottom panes of Fig. 8 shows the trajectory for five ions species with different mobility coefficients: $K(0) = 1.0, 1.5, 2.0, 2.5, 3.0\ \mathrm{cm^2\ V^{-1}\ s^{-1}}$ within a DMS analyzer ($H = 0.5$ mm) using a waveform generator operating at 600 kHz. The SV (1500 V) and CV (−25.5 V) were optimized for transmission of the ion displayed with the $K(0) = 3.0\ \mathrm{cm^2\ V^{-1}\ s^{-1}}$ (red trajectories), and the DMS electrodes are depicted in brown. The higher frequency (2.4 MHz) has a significantly smaller amplitude of oscillation, leading to lower wall losses and a higher coefficient of transmission. The modeling data shown in Fig. 8 indicate that improved transmission through a DMS cell can be achieved by supplying an asymmetric waveform at higher frequencies.

An experimental test of this frequency effect was performed with samples of leucine for asymmetric waveforms ranging from 750 kHz to 3 MHz. To obtain the experimental data, an asymmetric waveform generator was modified such that the operational frequency could be varied simply by replacing the coil boxes associated with each of the two harmonics. Leucine was selected for these experiments because it has a relatively high mobility and therefore showed losses due to electrode neutralization at the lowest frequencies. Initially, CV scans were conducted with both power supply coil configurations and the SV turned off. Under these condi-

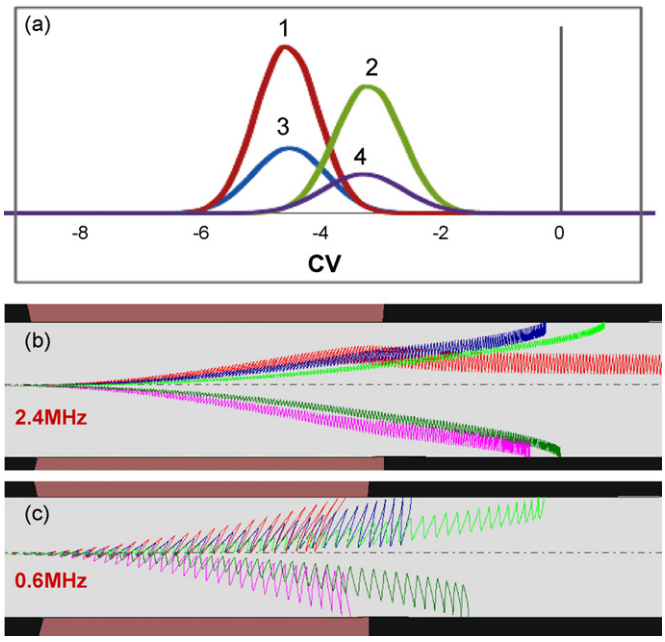


**Fig. 8.** SV frequency effect in DMS. The top pane (a) shows the experimental decrease in leucine ion signal when the SV frequency is reduced from 3 to 0.75 MHz, at SV peak-to-peak values of 3500 V (left pair of peaks, curves 1 and 3), and 3000 V (right peaks, curves 2 and 4). Middle (b) and bottom (c) panes show calculated trajectories for two different frequencies, also indicating that more ions can enter the DMS filter when the SV frequency is higher.

tions, the frequency of the power supply is irrelevant, and the peak intensity observed was the same for the two configurations. Leucine DMS spectra for SV amplitudes of 3000 and 3500 V are shown in the top pane of Fig. 8 for frequencies of 750 kHz and 3 MHz. The higher frequency configuration provided a sensitivity improvement over the lower frequency configuration, in agreement with the theoretical modeling. The observed gains were approximately 2.5× and 3.5× for operation at 3000 and 3500 V, respectively. Experiments with other low $m/z$ samples also demonstrated gains on the order of approximately 2× when operating at 3 MHz. The observed gain was reduced for lower mobility compounds.

## 4. Conclusions

We have shown that planar differential mobility spectrometry (DMS) is easily adapted for use as an ion-pre-filter for mass spectrometry, and provides the ability to separate a wide range of ion species for applications, providing reduced chemical noise, and improved quantitative accuracy. We have investigated differential mobility device characteristics, for both planar and cylindrical geometries for the purpose of optimizing the design for incorporation on a high sensitivity mass spectrometer. We have optimized ion transmission and transport efficiency, while providing resolution adjustable between high sensitivity and high resolution limits. DMS ion separation has exhibited stable operation under conditions of continuous high sample contamination and under long-term testing. Because the planar DMS design offers a transparent mode useful in the development of ion sources and sample handling protocols and has been found to be resistant to contamination, we expect it to be useful in many environments where high throughput needs to be combined with high quantitative accuracy.

## Acknowledgements

Many individuals have contributed to this work. Our thanks go to Stan Potyrala for the mechanical engineering of the prototype DMS cells and MS interface described. Electronics engineering design and support was provided by John Vandermey and Jeremy Corbeil.

This work was partially supported by the Columbia University Center for Medical Countermeasures against Radiation (P.I. David Brenner) and funded by NIH (NIAID) grant U19 AI067773-04.

## References

[1] E.V. Krylov, E.G. Nazarov, R.A. Miller, Differential mobility spectrometer: model of operation, Int. J. Mass Spectrom. 266 (2007) 76–85.
[2] G. Eiceman, Z. Karpas, Ion Mobility Spectrometry, second ed., CRC Press, Taylor & Francis LLC, Boca Raton, FL, 2005.
[3] A.A. Shvartsburg, Differential Ion Mobility: Non-linear Ion Transport and Fundamentals of FAIMS, CRC Group, Taylor & Francis LLC, Boca Raton, FL, 2008.
[4] M.P. Gorshkov, Inventor's certificate of USSR No. 966583, G01N27/62 (1982).
[5] A. Buryakov, E.V. Krylov, A.L. Makas, E.G. Nazarov, V.V. Pervukhin, U.Kh. Rasulev, Separation of ions according to mobility in a strong electric field, Sov. Tech. Phys. Lett. 17 (6) (1991) 446–447.
[6] I.A. Buryakov, E.V. Krylov, A.L. Makas, E.G. Nazarov, V.V. Pervukhin, U.Kh. Rasulev, Drift spectrometer for the control of amine traces in the atmosphere, J. Anal. Chem. [Zhurnal Analiticheskoi Khimii] 48 (2) (1993) 114–121.
[7] I.A. Buryakov, E.V. Krylov, E.G. Nazarov, U.Kh. Rasulev, A new method of separation of multi-atomic ions by mobility at atmospheric pressure using a high-frequency amplitude-asymmetric strong electric field, Int. J. Mass Spectrom. Ion Process. 128 (1993) 143–148.
[8] A.L. Makas, E.G. Nazarov, V.V. Pervukhin, U.Kh. Rasulev, Mass spectrometric investigation of the surface ionization of organic compounds at atmospheric pressure, Sov. Tech. Phys. Lett. 16 (6) (1990) 458–460.
[9] R.A. Miller, E.G. Nazarov, G.A. Eiceman, A.T. King, A MEMS radio-frequency ion mobility spectrometer for chemical vapor detection, Sens. Actuators A 91 (2001) 301–312.
[10] R.A. Miller, G.A. Eiceman, E.G. Nazarov, A.T. King, A novel micromachined high-field asymmetric waveform-ion mobility spectrometer, Sens. Actuators B 67 (2000) 300–306.
[11] E.V. Krylov, High voltage pulse generator, Instrum. Exp. Tech. 4 (1991) 114–115.
[12] E.V. Krylov, Pulses of special shapes formed on a capacitive load, Instrum. Exp. Tech. 5 (1997) 47–50.
[13] B. Carnahan, S. Day, V. Kouznetsov, A. Tarassov, Development and applications of transverse field compensation ion mobility spectrometer, in: Proceeding of an Fourth International Workshop on Ion Mobility Spectrometry, Cambridge, UK, 1995.
[14] B. Carnahan, S. Day, V. Kouznetsov, M. Matyjaszczyk, A. Tarassov, Field ion spectrometry—a new analytical technology for trace gas analysis, in: Proceedings of the 41st Annual ISA Analysis Division Symposium, vol. 51(1), Framingham, MA, April 21–24, 1996, pp. 87–96.
[15] A.N. Verenchikov, E.V. Krylov, V.B. Louppou, A.L. Makas, V.V. Pervukhin, V.A. Shkurov, Analysis of ionic compositions of solutions using an ion gas analyzer, in: V.V. Malakhov (Ed.), Chemical Analysis of Environment, Nauka, Novosibirsk, 1991, pp. 127–133.
[16] R.W. Purves, R. Guevremont, Electrospray ionization-high asymmetric waveform ion mobility spectrometry–mass spectrometry, Anal. Chem. 71 (1999) 2346–2357.
[17] G.A. Eiceman, E.G. Nazarov, R.A. Miller, Micro-machined ion mobility spectrometer-mass spectrometer, Int. J. Ion Mobil. Spec. 3 (1) (2000) 15–27.
[18] D.S. Levin, P. Vouros, R.A. Miller, E.G. Nazarov, J.C. Morris, Characterization of gas phase molecular interactions on differential mobility ion behavior utilizing an electrospray ionization differential mobility mass spectrometry system, Anal. Chem. 78 (2006) 96–106.
[19] A.A. Shvartsburg, F. Li, K. Tang, R.D. Smith, High-resolution field asymmetric waveform ion mobility spectrometry using new planar geometry analyzers, Anal. Chem. 78 (2006) 3706–3714.
[20] R.W. Purves, R. Guevremont, Mass-spectrometric characterization of a high-field asymmetric waveform ion mobility spectrometer, Rev. Sci. Instrum. 69 (1999) 4094–4105.
[21] G. Eiceman, Z. Karpas, Ion Mobility Spectrometry, first ed., CRC Press, Taylor & Francis LLC, Boca Raton, FL, 1993.
[22] H.E. Revercomb, E.A. Mason, Theory of plasma chromatography/gaseous electrophoresis—a review, Anal. Chem. 47 (7) (1975) 970–983.
[23] T.W. Carr, Plasma Chromatography, Plenum Press, New York, 1984.
[24] E.A. Mason, E.W. McDaniel, Transport Properties of Ions in Gases, John Wiley & Sons, NY, 1988.
[25] R.R. Landgraf, C.K. Hilton, R.A. Yost, Effect of carrier gas composition in ESI-FAIMS/MS on separation of charge states and conformers of intact proteins, in: 54th ASMS Conference Proceedings, 2006.
[26] D.S. Levin, R.A. Miller, E.G. Nazarov, P. Vouros, Rapid separation and quantitative analysis of peptides using a new nanoelectrospray-differential mobility spectrometer–mass spectrometer system, Anal. Chem. 78 (2006) 5443–5452.
[27] D.S. Levin, P. Vouros, R.A. Miller, E.G. Nazarov, Using a nanoelectrospray-differential mobility spectrometer system for the analysis of oligosaccharides with solvent selected control over ESI aggregate ion formation, Am. Soc. Mass Spectrom. 18 (2007) 502–511.
[28] I.V. Chernushevich, W. Ens, K.G. Standing, Orthogonal injection TOF MS for analyzing biomolecules, Anal. Chem. 71 (1999) 452A–461A.
[29] A.B. Kanu, P. Dwivedi, M. Tarm, L. Matz, H.H. Hill, Ion mobility–mass spectrometry, J. Mass Spectrom. 43 (2008) 1–22.
[30] E.V. Krylov, A method of reducing diffusion losses in a drift spectrometer, Tech. Phys. Am. Inst. Phys. 44 (1) (1999) 113–136.
[31] R. Guevremont, R.W. Purves, Atmospheric pressure ion focusing in a high field asymmetric waveform ion mobility spectrometer, Rev. Sci. Instrum. 70 (1999) 1370–1383.
[32] B.B. Schneider, T.R. Covey, S.L. Coy, E.V. Krylov, E.G. Nazarov, Control of chemical effects in the separation process of a DMS/MS system, Eur. J. Mass Spectrom. 16 (2010) 57–71.
[33] E.V. Krylov, S.L. Coy, J. Vandermey, B.B. Schneider, T.R. Covey, E.G. Nazarov, Selection and generation of waveforms for differential mobility spectrometry, Rev. Sci. Inst. 81 (2010) 1, doi:10.1063/1.3284507.
[34] V. Kouznetsov, High voltage waveform generator, U.S. Patent 5,801,379 (1998).
[35] M. Jugroot, C.P.T. Groth, B.A. Thomson, V. Baranov, B.A. Collings, Numerical investigation of interface region flows in mass spectrometers: ion transport, J. Phys. D: Appl. Phys. 37 (2004) 550–559.
[36] E.G. Nazarov, R.A. Miller, S.L. Coy, E. Krylov, S.I. Kryuchkov, Software simulation of ion motion in DC and AC electric fields including fluid-flow effects. (SIONEX microDMx SOFTWARE), Int. J. Ion Mobil. Spec. 9 (1) (2006) 35–39.
[37] E.V. Krylov, Ion Mobility in Gases in a Moderate Strength Electric Fields, PhD Thesis, St.-Petersburg Polytechnic University, St.-Petersburg, Russia, 1995.
[38] A. Kudryavtsev, A. Makas, Ion focusing in an ion mobility increment spectrometer (IMIS) with non-uniform electric fields: fundamental considerations, Int. J. Ion Mobil. Spec. 4 (2) (2001) 117–120.
[39] I.A. Buryakov, Ion mobility increment spectrometer with radial symmetry, Int. J. Ion Mobil. Spec. 6 (2003) 1–7.
[40] B.B. Schneider, H. Javaheri, T.R. Covey, Ion sampling effects under conditions of total solvent consumption, Rapid Commun. Mass Spectrom. 20 (2006) 1538–1544.